DOI: 10.1021/cg1005693

CRYSTAL GROWTH & DESIGN Article

2010, Vol. 10
3732–3742

Co-Crystals of Active Pharmaceutical Ingredients - Acetazolamide

Jenniffer I. Arenas-García,[†] Dea Herrera-Ruiz,*[,†] Karina Mondragón-Vásquez,[‡] Hugo Morales-Rojas,[‡] and Herbert Höpfl*[,‡]

[†]*Facultad de Farmacia, Universidad Autónoma del Estado de Morelos, Av. Universidad 1001, C.P. 62209 Cuernavaca, México, and* [‡]*Centro de Investigaciones Químicas, Universidad Autónoma del Estado de Morelos, Av. Universidad 1001, C.P. 62209 Cuernavaca, México*

Received April 28, 2010; Revised Manuscript Received June 13, 2010

ABSTRACT: A total of 20 co-crystal formers have been combined with acetazolamide (ACZ) via solvent drop grinding in acetone, acetonitrile, and water. The screening experiments provided co-crystals with 4-hydroxybenzoic acid (4HBA) and nicotinamide (NA) (**ACZ-4HBA** and **ACZ-NA-H_2O**), which were identified by X-ray powder diffraction (XRPD) and further characterized by IR spectroscopy and differential scanning calorimetry-thermogravimetric analysis (DSC-TGA). Both co-crystals could be prepared also by neat grinding (NG) and reaction crystallization (RC). Single-crystal X-ray diffraction analyses allowed for an examination of the dominant hydrogen bonding patterns in the co-crystals, showing that 4HBA binds to the thiadiazole acetamide fragment of ACZ via C(N)NH···HOOC and O−H···N interactions, while NA is linked through N−H···N and N−H···O contacts. In **ACZ-NA-H_2O**, the components are connected further by crystal lattice water molecules through N−H···O_w and O_w−H···N hydrogen bonds. Phase stability assays in water at physiological pH values ranging from 1.2 to 6.8 showed that for **ACZ-4HBA** the crystalline solid phase did not transform to ACZ within 72 h, while for **ACZ-NA-H_2O** a gradual transformation occurred. Thermal treatment of **ACZ-NA-H_2O** and reaction crystallization experiments in methanol and anhydrous ethanol gave the dehydrated crystalline phase **ACZ-NA**, which is stable at ambient conditions for at least four months but transforms to the corresponding co-crystal monohydrate when stirred with deionized water.

1. Introduction

Most medicaments contain active pharmaceutical ingredients (APIs) in the solid form. For commercial purposes, crystalline forms are strongly preferred because they tend to be more stable, reproducible, and amenable to purification than other types of solids.[1]

The arrangement of molecules in the crystalline state affects physical and chemical properties on the macroscopic level, and variations in the structural organization can influence the efficacy and bioavailability of the drug.[1,2] Most of the strategies to improve the biopharmaceutical properties of a drug, such as solubility, dissolution rate, chemical stability, and hygroscopicity, focus on the preparation of amorphous solids, polymorphs, solvates, salts,[1,2] and, more recently, co-crystals.[1,3,4] According to Zawarotko's definition, a co-crystal is a compound made from reagents that are solids at ambient temperature[3a] and can be designed by crystal engineering[5] with the intention to improve the solid-state properties of an active pharmaceutical ingredient (API) without affecting its intrinsic structure. Co-crystals are endowed with particular scientific[1,3,4] and regulatory advantages[6] which confer them great opportunities and challenges.

Acetazolamide (ACZ), 5-acetamido-1,3,4-thiadiazole-2-sulfonamide, is an inhibitor of carbonic anhydrase and is used mainly for the treatment of glaucoma.[7] It has been considered also as an antiepileptic and diuretic agent, for treating acute high altitude sickness, and most recently has been evaluated as a remedy against respiratory diseases and to prevent adverse effects of drugs in the treatment of influenza.[8] ACZ has a pK_a value of 7.2, and so far, two structurally characterized polymorphic forms of ACZ are known (forms A and B), form A being the more stable solid phase at room temperature.[9,10]

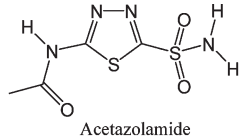

Acetazolamide

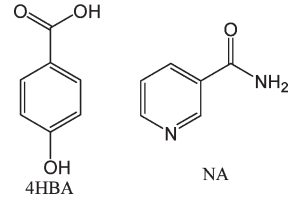

4HBA NA

By virtue of the fact that acetazolamide has low solubility (0.72 mg/mL in water at 25 °C) and permeability, the discovery and identification of new solid forms of ACZ is relevant to improve its physical and/or chemical properties.[8a,10] Hence, in this work we report on new solid-state phases of acetazolamide in the form of co-crystals that potentially present advantages over the medicament in its actual commercially available presentations. Additionally, four different methods of co-crystal preparation have been examined and preliminary studies have been carried out concerning thermal stability and co-crystal phase stability in the presence of water.

2. Experimental Section

Materials. Acetazolamide (form A), co-crystal formers, and solvents were commercially available and were used as received without further purification.

*To whom correspondence should be addressed. (D.H.-R.) E-mail: dherrera@uaem.mx. (H.H.) Fax: (+52) 77-73-29-79-97. E-mail: hhopfl@ciq.uaem.mx.

Published on Web 06/29/2010

Co-Crystal Screening of Acetazolamide. Solvent drop grinding (SDG) experiments were performed by combining equimolar ratios of ACZ and the corresponding co-crystal former. These mixtures were then placed into stainless steel grinding jars (1.5 mL), and one drop of acetone, acetonitrile, or water was added to the compound mixture before starting mechanical grinding in a Retsch MM400 mixer mill for 30 min at 25 Hz, using one stainless steel grinding ball. The solid phases were then characterized by X-ray powder diffraction (XRPD).

Neat Grinding and Reaction Crystallization Experiments. Neat grinding (NG) experiments were performed with the same equipment in an analogous manner, but without solvent and enhancing the duration of the mechanical grinding to 60 min. For the reaction crystallization (RC) experiment with 4-hydroxybenzoic acid (4-HBA) as co-crystal former, a saturated solution of 4-HBA in THF was heated to 50 °C, whereupon small quantities of ACZ were added until a white powder was observed. For the preparation of **ACZ-NA-H_2O**, nicotinamide (NA) was dissolved in water or solvent mixtures of acetonitrile, acetone, or methanol with water (in each case, 75/25, 50/50, and 25/75 vv) to prepare a saturated solution, which was heated to 90 °C. Then, small quantities of ACZ were added until a white powder was observed. When using methanol or anhydrous ethanol as solvent, water-free **ACZ-NA** was obtained. In all cases, after precipitation was initiated the solutions were cooled down slowly to room temperature and stirred for 8 h. The precipitates formed were filtered and characterized by XRPD.

Single-Crystal Growth. Co-crystals were grown also by slow evaporation experiments.

Acetazolamide-4-Hydroxybenzoic Acid 1:1 (ACZ-4HBA). 1:1, 1:3, and 1:5 stoichiometric ratios of the starting materials were dissolved in hot acetonitrile. A mixture of single crystals of **ACZ** and **ACZ-4HBA** co-crystals were obtained after three days by slow solvent evaporation at room temperature from the 1:3 mixture. The 1:1 and 1:5 mixtures provided only crystals of ACZ.

Acetazolamide-Nicotinamide-H_2O 1:1:1 (ACZ-NA-H_2O). 1:0.5, 1:1, 1:1.5, 1:2, 1:3, 1:4, 1:5, and 1:10 stoichiometric ratios of ACZ and nicotinamide (NA) were employed to crystallize the sample from hot water in the presence of small quantities of the compound previously obtained by grinding (seeding). Large single-crystals of **ACZ-NA-H_2O** formed after three months by slow solvent evaporation at room temperature from the 1:4 mixture.

Nicotinamide-4-Hydroxybenzoic Acid 1:1 (NA-4HBA). A 1:1 mixture of nicotinamide and 4-hydroxybenzoic acid was dissolved in acetone. Single crystals were obtained in pure form by slow evaporation of the solution.

Co-Crystal Phase Stability Tests. 100 μL of deionized water were added to 25 mg of co-crystal. After the suspension was stirred for 16 or 72 h, the resulting solid was filtered under a vacuum and characterized by XRPD. In a similar manner, experiments using buffer solutions adjusted to pH values of 1.2 (hydrochloric acid solution, 0.034 M), 4.5 (phosphate buffer solution, 0.1 M), and 6.8 (phosphate buffer solution, 0.05 M) were accomplished.

Instrumental. IR spectra were recorded on a Bruker Vector 22 FT spectrophotometer and measured in the range of 4000−400 cm^{-1} using the KBr pellet technique. Differential scanning calorimetry (DSC) and thermogravimetric analyses (TGA) were accomplished with a TA SDT Q600 instrument. Approximately 3 mg of each solid sample were placed in alumina crucibles and analyzed in the temperature range of 50−400 °C with a 10 °C/min heating rate, using a current of 50 mL/min of nitrogen as inert gas purge.

X-ray Diffraction Analysis. XRPD analyses were carried out in the transmission mode on a BRUKER D8-ADVANCE diffractometer equipped with a LynxEye detector ($\lambda_{Cu-K\alpha 1}$ = 1.5406 Å, monochromator: germanium). Data were collected at room temperature in the range of 2θ = 5−40 or 5−50° (step size 0.011°, step times 0.30 and 10 s). Single-crystal X-ray diffraction studies were performed on a Bruker-APEX diffractometer with a CCD area detector ($\lambda_{MoK\alpha}$ = 0.71073 Å, monochromator: graphite). Frames were collected at T = 100 K (compounds **ACZ-4HBA**, **ACZ-NA-H_2O**, and **NA-4HBA**) and T = 293 K (compounds **ACZ-4HBA** and **ACZ-NA-H_2O**) via ω/ϕ-rotation at 10 s per frame (SMART).[11a] The measured intensities were reduced to F^2 and corrected for absorption with SADABS (SAINT-NT).[11b] Corrections were made for Lorentz and polarization effects. Structure solution, refinement, and data output were carried out with the SHELXTL-NT program package.[11c,d] Non-hydrogen atoms were refined anisotropically. C−H hydrogen atoms were placed in geometrically calculated positions using a riding model. O−H and N−H hydrogen atoms were localized by difference Fourier maps and refined fixing the bond lengths to 0.84 and 0.86 Å, respectively; the corresponding isotropic temperature factors have been fixed to a value 1.5 times that of the corresponding oxygen/nitrogen atoms. Figures were created with SHELXTL-NT.[11c,d] Hydrogen-bonding interactions in the crystal lattice were calculated with the WINGX program package.[12] Crystallographic data for the five crystal structures were deposited with the Cambridge Crystallographic Data Centre as supplementary publications no. CCDC-773415−773419. Copies of the data can be obtained free of charge on application to CCDC, 12 Union Road, Cambridge CB2 1EZ, UK (fax: (+44) 1223-336-033; e-mail: deposit@ccdc.cam.ac.uk, www: http://www.ccdc.cam.ac.uk).

Scheme 1. Homo- and Heterodimeric Synthons Formed between Carboxylic Acids, Carboxamides, Carboxamidines, and Sulfonamides

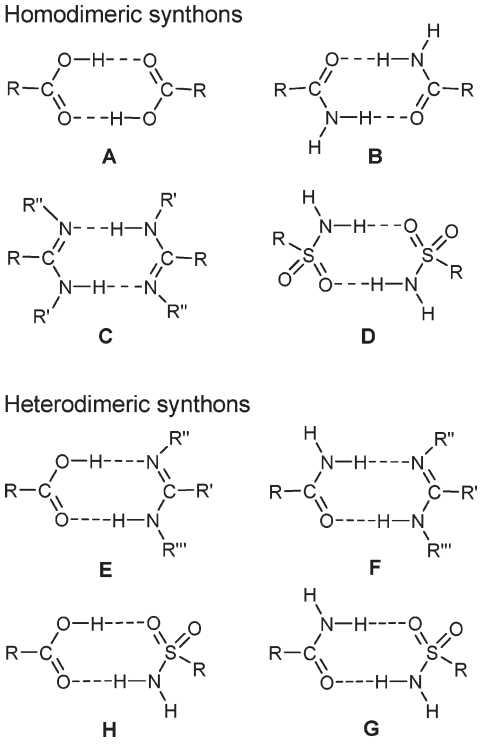

3. Results and Discussion

Screening Experiments. In the crystal structures of both polymorphs reported so far for ACZ, the molecules are linked through double-bridged homodimeric C(N)NH···HN(N)C synthons (motif **C** in Scheme 1) and N−H···O interactions between the sulfonamide groups. However, only one of the two polymorphs (form A) contains the homodimeric sulfonamide···sulfonamide synthon **D** (vide infra).[9a,c,d] Because of the structural relationship of these functions with carboxamide and carboxylic acid homodimers (motifs **A** and **B**), we have chosen mainly carboxylic acids and carboxamides as co-crystal formers for the experiments performed herein with the hypothesis that the formation of dimeric heterosynthons **E-H** (Scheme 1) might induce co-crystallization. Furthermore, many of these derivatives are members of the GRAS list[13] and have been employed previously for co-crystallization experiments with APIs.[3,4] Co-crystals of APIs with nicotinamide and 4-hydroxybenzoic acid as co-crystal formers have

Table 1. Results of the Screening Experiments for the Formation of Co-Crystals with Acetazolamide

Co-crystal former	Stoichiometry ACZ/Co-crystal former	Solvents C_3H_6O	CH_3CN	H_2O	Co-crystal former	Stoichiometry ACZ/Co-crystal former	Solvents C_3H_6O	CH_3CN	H_2O
Oxalic acid 	1:1	X	X	X	2,5-dihydroxy-benzoic acid 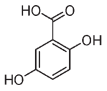	1:1	X	X	X
Malonic acid 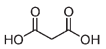	1:1	X	X	X	4-hydroxybenz-amide 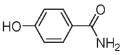	1:1	X	X	Co-crystal former hydrate
Succinic acid 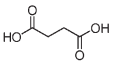	1:1	X	X	X	Picolinic acid 	1:1	X	X	X
Glutaric acid 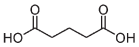	1:1	X	X	X	Nicotinic acid 	1:1	X	X	X
Adipic acid 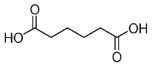	1:1	X	X	X	Isonicotinic acid 	1:1	X	X	X
Camphoric acid 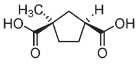	1:1	X	X	X	2-hydroxynicotinic acid 	1:1	X	X	X
Citric acid 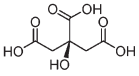	1:1	X	X	X	Nicotinamide 	1:1 2:1[a] 1:2[a]	X	X	✓
Benzoic acid 	1:1	X	X	X	Isonicotinamide 	1:1	X	X	Co-crystal former hydrate
Salicylic acid 	1:1	X	X	X	Saccharine 	1:1	X	X	X
4-hydroxybenzoic acid 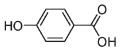	1:1 2:1[a] 1:2[a]	✓	✓	✓	Caffeine 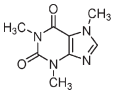	1:1	X	X	X

[a]1:2 and 2:1 grinding experiments showed that only the 1:1 co-crystal is formed under these conditions, since additionally only peaks for the unreacted reagent in excess were observed.

been reported for caffeine,[14] carbamazepine,[15] celecoxib,[16] ethyl paraben,[17] ibuprofen,[15e,18] piracetam,[3c] piroxicam,[15a,19] and theophylline.[20]

A total of 20 co-crystal formers were employed in the screening experiments using the solvent drop grinding (SDG) method.[21] For this purpose, three solvents of different polarity were chosen: acetone, acetonitrile, and water. Novel solid phases were identified by XRPD, and to discriminate co-crystals from polymorphs or solvates, parallel grinding experiments were performed using only ACZ or the corresponding co-crystal former with the respective solvent. This procedure allowed us to establish that the solid phases obtained with 4-hydroxybenzamide and isonicotinamide contained only the monohydrate of the corresponding co-crystal former[22] and ACZ.

The formation of 1:1 co-crystals was confirmed also by comparison with the XRPD patterns resulting from 1:2 and 2:1 grinding experiments, showing for all co-crystals described herein in the first case peaks of unreacted co-crystal former and in the second case peaks of unreacted ACZ. The co-crystals were further characterized by DSC-TGA, IR spectroscopy, and single-crystal X-ray diffraction analysis, showing that 4HBA generated pharmaceutical 1:1 co-crystals, while NA gave a 1:1:1 co-crystal hydrate. The results of the screening experiments are summarized in Table 1.

XRPD Analysis. A comparison of the XRPD patterns given for **ACZ**, **4HBA**, and the solid obtained from the solvent drop grinding (SDG) experiment in acetonitrile indicates the formation of a solid phase different from the starting materials (Figure 1a−d). The same phase was obtained using acetone

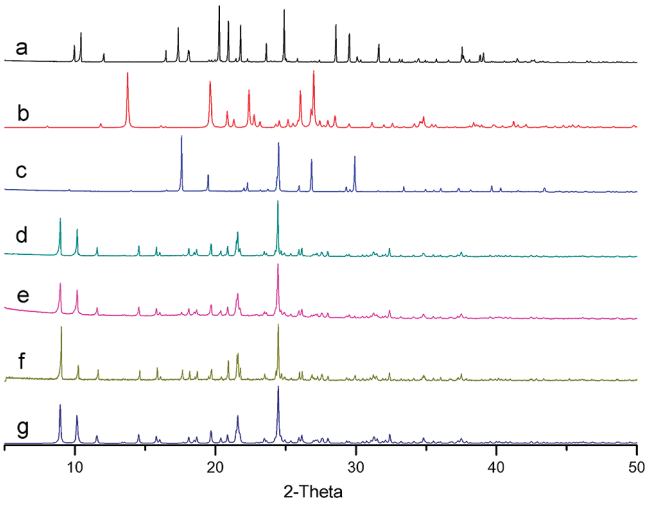

Figure 1. XRPD patterns of (a) **ACZ** form A, (b) **ACZ** form B, (c) **4HBA**, (d) co-crystals **ACZ-4HBA** obtained by SDG with acetonitrile, (e) co-crystals **ACZ-4HBA** obtained by NG, and (f) co-crystals **ACZ-4HBA** obtained by RC in THF. (g) Pattern calculated from the single-crystal X-ray diffraction analysis.

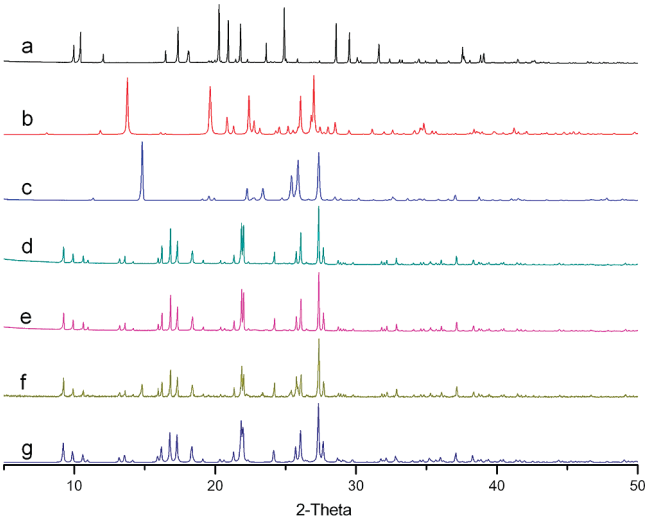

Figure 2. XRPD patterns of (a) **ACZ** form A, (b) **ACZ** form B, (c) **NA**, (d) co-crystals **ACZ-NA-H_2O** obtained by SDG with H_2O, (e) co-crystals **ACZ-NA-H_2O** obtained by NG, and (f) co-crystals **ACZ-NA-H_2O** obtained by RC in a solvent mixture of acetonitrile and water (50/50 vv). (g) Pattern calculated from the single-crystal X-ray diffraction analysis.

and water as solvents. In view of the formation of a new phase, additionally neat grinding (NG)[3f] and reaction crystallization (RC) experiments[3f,15b] were carried out, showing that the same phase also can be formed in the absence of solvent and via reaction precipitation in THF (Figure 1e,f). Comparison of the corresponding diffraction patterns with that calculated from the single-crystal data of **ACZ-4HBA** (Figure 1g) show further that the crystalline compound obtained by slow solvent evaporation is identical to the products formed by the above-mentioned methods.

With NA a new solid phase was observed only for the SDG experiment using water, thus indicating that a hydrate had formed (**ACZ-NA-H_2O**), which was further evidenced by TGA and single-crystal X-ray diffraction analysis. Interestingly, the co-crystal also could be prepared by the NG method, indicating that the sample mixture incorporated water from the

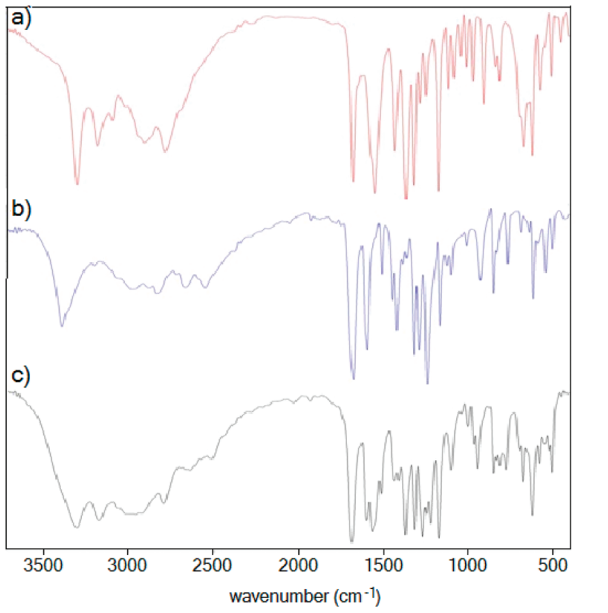

Figure 3. Infrared spectra of (a) **ACZ**, (b) **4HBA**, and (c) **ACZ-4HBA**.

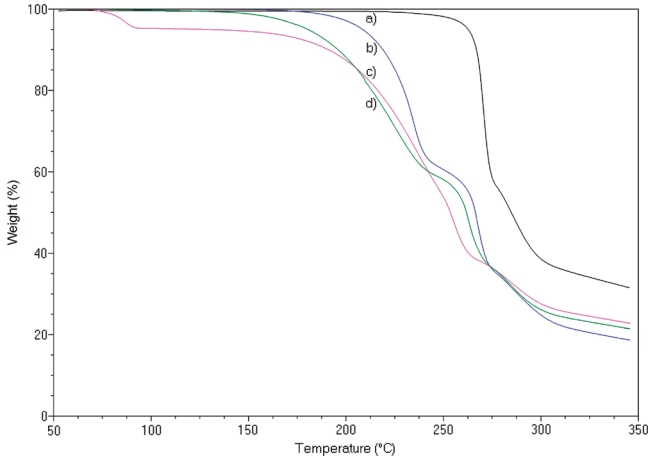

Figure 4. TGA graphs of (a) **ACZ**, (b) **ACZ-4HBA**, (c) **ACZ-NA-H_2O**, and (d) **ACZ-NA**.

atmosphere (Figure 2). For a successful performance of the RC method, in this case a hot solvent mixture containing a significant amount of water was required, that is, 75/25, 50/50, or 25/75 vv mixtures of water with acetonitrile, acetone, or methanol. The product also can be prepared from hot water alone (90 °C); however, because of the low solubility of ACZ in this solvent, only very small quantities were obtained.

IR Spectroscopy. IR spectroscopy is a valuable supplementary tool for the identification of new solid forms. Figure 3 shows the IR spectra of **ACZ**,[9b,e] co-crystal former **4HBA**, and co-crystal **ACZ-4HBA**. The corresponding IR spectra for **ACZ-NA-H_2O** are shown in the Supporting Information (Figure S1). A listing of the most characteristic IR bands of all co-crystals examined herein is given in Table 2, together with the data for **ACZ** and the corresponding co-crystal formers.

For both co-crystals the resulting spectra are different from superimposed spectra of the starting materials, and broad bands in the region of 2500−3500 cm^{-1} are observed, which are typical for crystal structures with extended hydrogen bonding interactions.[23] Furthermore, the presence of ACZ in the solid phases of

Table 2. Relevant Bands in the IR Spectra of ACZ, 4HBA, NA, and the Co-Crystals Examined Herein

	ACZ	4HBA	NA	ACZ-4HBA	ACZ- NA-H_2O	ACZ- NA	NA-4HBA
ν C=O	1680	1677	1679	1686	1680	1681	1672
ν OH, N−H	3302	3391	3368	3303	3450	3445	3436
	3182		3162	3173	3305	3161	3359
					3242		3194
ν N−H_{II}	1551[a]			1567[a]	1562[a]	1553[a]	
			1619[b]		1609[b]		1594[b]
ν SO_2NH_2	1368			1371	1355	1361	
	1177			1174	1172	1167	

[a] ν N−H_{II} for **ACZ**. [b] ν N−H_{II} for **NA**.

Table 3. DSC-TG Analyses of ACZ, 4HBA, NA, Co-Crystals

compound	mp (rep.) [°C][a]	mp [°C]	TGA mass loss before melting [%]	TGA solvent evap. [°C]
ACZ	258−259 (dec.)[b]	270 (dec.)[b]	0	
4HBA	213-217	212	0	
NA	128−131	131	0	
ACZ-4HBA		235 (dec.)	0	
ACZ-NA-H_2O		154	4.8	75
ACZ-NA		147	0	
NA-4HBA		185 (dec.)	0	

[a] Reported by Sigma-Aldrich. [b] The melting point of ACZ depends among others on the temperature of initial heating and the heating rate, mainly because ACZ starts to decompose above 255 °C. The reported melting points of ACZ vary from 250 to 270 °C.[9c]

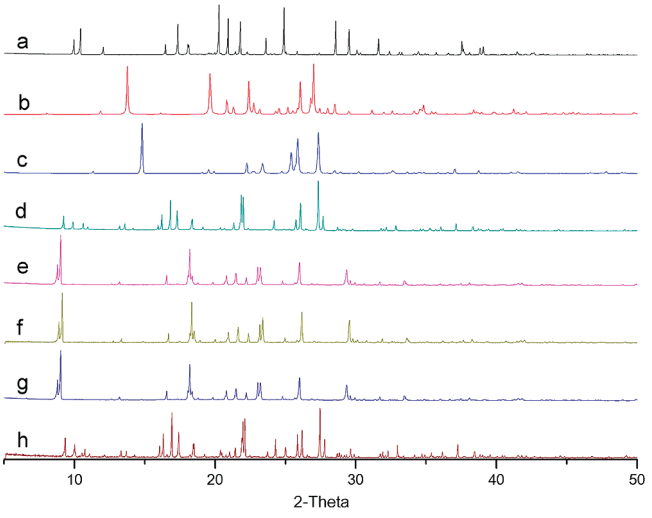

Figure 5. XRPD patterns of (a) **ACZ** form A, (b) **ACZ** form B, (c) **NA**, (d) co-crystals **ACZ-NA-H_2O** obtained by SDG with H_2O, (e) co-crystals **ACZ-NA** obtained after thermal treatment (75 °C for a period of 30 min), (f) co-crystals **ACZ-NA** obtained by RC in methanol, (g) co-crystals **ACZ-NA** after storage at ambient conditions (capped vial) for four months, and (h) co-crystals **ACZ-NA** after exposition to water for 16 h.

ACZ-4HBA and **ACZ-NA-H_2O** can be deduced from two characteristic bands for vibrations of the sulfonamide group in the region of 1355−1371 and 1167−1177 cm^{-1} (Table 2).[23]

The IR spectra allow the differentiation also between salts and co-crystals, which differ by the location of the proton between the acid and the base.[20,24] The infrared spectrum of **4HBA** shows a C=O stretching band at 1677 cm^{-1}. Since there was no significant shift to lower wavenumbers for **ACZ-4HBA**, a proton transfer from the coformer to ACZ did not occur (Figure 3). Arylcarboxylate salts generally show a strong band for the asymmetric ν_{COO} vibration in the range of 1610−1550 cm^{-1}.[23] That **ACZ-4HBA** is a

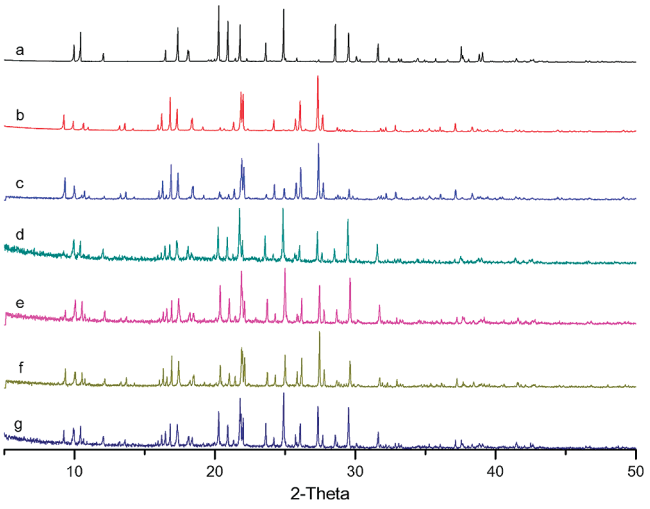

Figure 6. XRPD patterns of (a) **ACZ** and (b) co-crystal **ACZ-NA-H_2O** prepared by SDG with water, and after co-crystal phase stability tests (c) in water for 16 h, (d) in water for 72 h and for 72 h: (e) at pH 1.2, (f) at pH 4.5, (g) at pH 6.8.

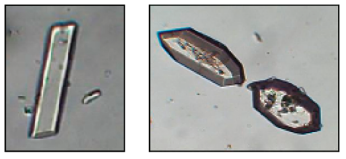

Figure 7. Crystals of acetazolamide (**ACZ**) and the corresponding co-crystal with 4-hydroxybenzoic acid (**ACZ-4HBA**) can be distinguished by their different shapes.

co-crystal rather than a salt was confirmed also by subsequent single-crystal X-ray diffraction analysis (vide infra).

DSC-TG Analysis. The TGA and DSC curves of **ACZ** and co-crystals **ACZ-4HBA** and **ACZ-NA-H_2O** are shown in Figures 4a−c and S2−S4. Table 3 summarizes the most relevant data of the DSC-TG analysis. The thermal profile of **ACZ-4HBA** reveals an endothermic peak at 235 °C which can be associated with starting decomposition. This value is different from those observed in the DSC-TGA curves of acetazolamide (270 °C) and 4-hydroxybenzoic acid (212 °C), confirming the formation of a new solid phase. The thermal curve of **ACZ-NA-H_2O** indicates a mass loss of 4.8% starting at 75 °C, which is in accordance with the presence of solvent (water) in the sample (calc.: 4.97%). Fusion of the residual solid occurs at 154 °C, a temperature lying between the melting points of **ACZ** (270 °C) and **NA** (131 °C). After fusion, the compound starts to decompose.

Formation of Co-Crystal ACZ-NA. The TGA experiment of **ACZ-NA-H_2O** suggests that the crystal lattice water molecules

Table 4. Crystallographic Data for Compounds ACZ-4HBA, ACZ-NA-H_2O, and NA-4HBA

crystal data[a]	**ACZ-4HBA** (100 K)	**ACZ-4HBA** (293 K)	**ACZ-NA-H_2O** (100 K)	**ACZ-NA-H_2O** (293 K)	**NA-4HBA** (100 K)
formula	$C_4H_6N_4O_3S_2 \cdot C_7H_6O_3$	$C_4H_6N_4O_3S_2 \cdot C_7H_6O_3$	$C_4H_6N_4O_3S_2 \cdot C_6H_6N_2O \cdot H_2O$	$C_4H_6N_4O_3S_2 \cdot C_6H_6N_2O \cdot H_2O$	$C_6H_6N_2O \cdot C_7H_6O_3$
MW (g mol^{-1})	360.37	360.37	362.39	362.39	260.25
space group	$P2_1/c$	$P2_1/c$	$P\bar{1}$	$P\bar{1}$	$C2/c$
temp (K)	100(2)	293(2)	100(2)	293(2)	100(2)
a (Å)	9.8604(11)	10.0472(15)	8.1739(13)	8.3077(14)	30.839(5)
b (Å)	17.317(2)	17.417(3)	9.8875(16)	9.9633(17)	7.2117(11)
c (Å)	8.6148(10)	8.6623(13)	10.3940(17)	10.4596(18)	11.1457(17)
α (°)	90	90	66.946(2)	66.601(2)	90
β (°)	99.901(2)	100.733(3)	84.672(3)	83.567(3)	107.561(2)
γ (°)	90	90	77.519(2)	76.787(3)	90
V (Å^3)	1449.1(3)	1489.3(4)	754.7(2)	773.3(2)	2363.3(6)
Z	4	4	2	2	8
μ (mm^{-1})	0.406	0.395	0.389	0.380	0.110
ρcalcd (g cm^{-3})	1.652	1.607	1.595	1.556	1.463
$R^{b,c}$	0.040	0.041	0.035	0.038	0.051
$R_w{}^{d,e}$	0.092	0.102	0.093	0.100	0.116

[a] $\lambda_{MoK\alpha}$ = 0.71073 Å. [b] $F_o > 4\sigma(F_o)$. [c] $R = \Sigma||F_o| - |F_c||/\Sigma|F_o|$. [d] All data. [e] $R_w = [\Sigma w(F_o^2 - F_c^2)^2/\Sigma w(F_o^2)^2]^{1/2}$.

Scheme 2. Hydrogen Bonding Motifs Identified in the Crystal Structures of Co-Crystals ACZ-4HBA (Motifs I−IV), ACZ-NA-H_2O (Motifs V−VIII), and NA-4HBA (Motifs IX−X)

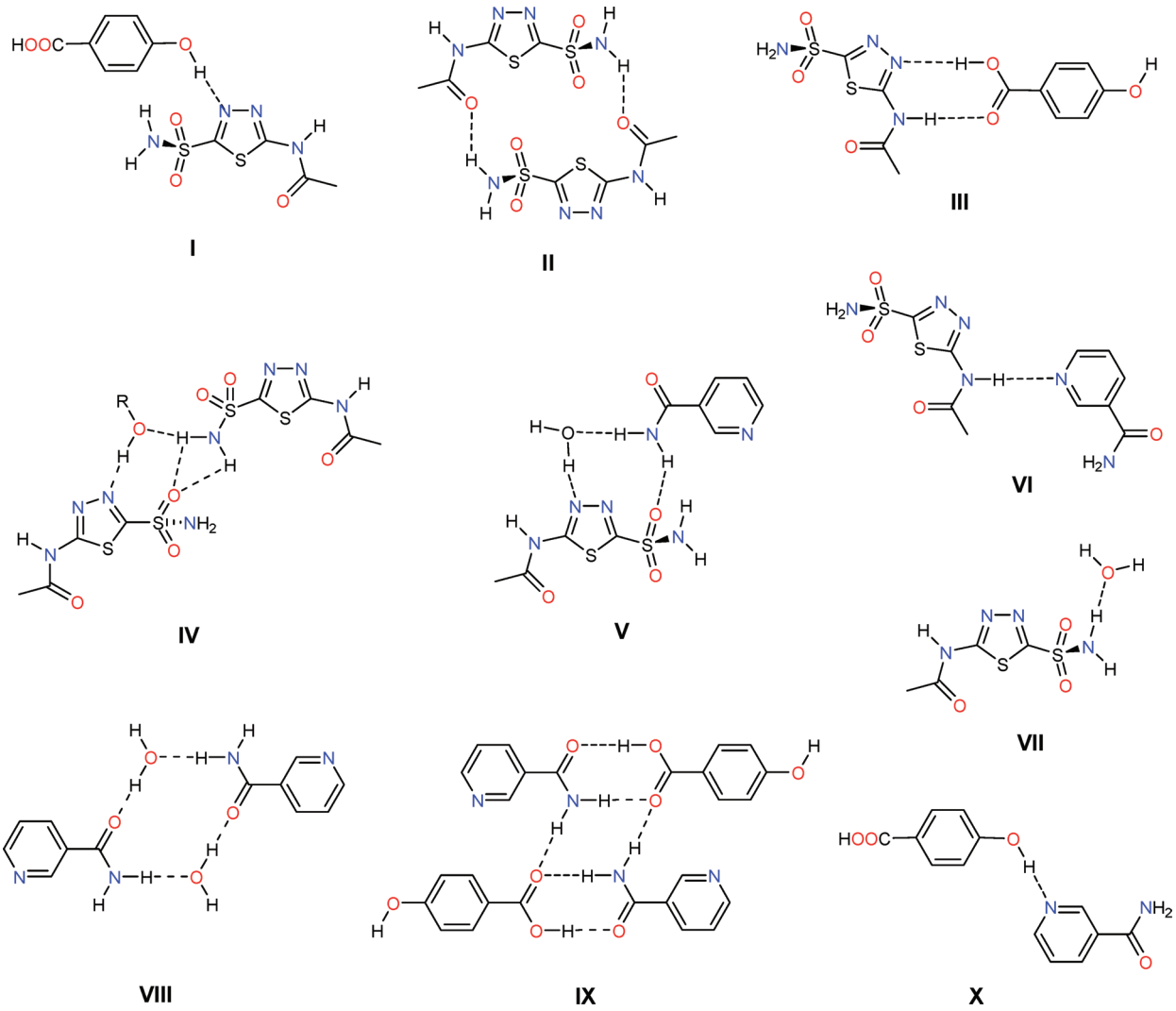

can be eliminated through thermal treatment. Indeed, after heating the co-crystal monohydrate to either 75 °C for a period of 30 min or 100 °C for 10 min, a new solid phase was obtained as shown by a comparison of the XRPD patterns (Figure 5). The same crystalline phase could be obtained also with the RC method using methanol or anhydrous ethanol as solvent, whereas from THF, acetonitrile, and acetone only ACZ precipitated. That this new phase is a co-crystal can be seen from a comparison of the IR data given in Table 2 and Figure S5, which shows the presence of both ACZ and NA. The TGA graph in Figure 4d shows that the co-crystal is water-free, so that the composition **ACZ-NA** can be proposed, which is further

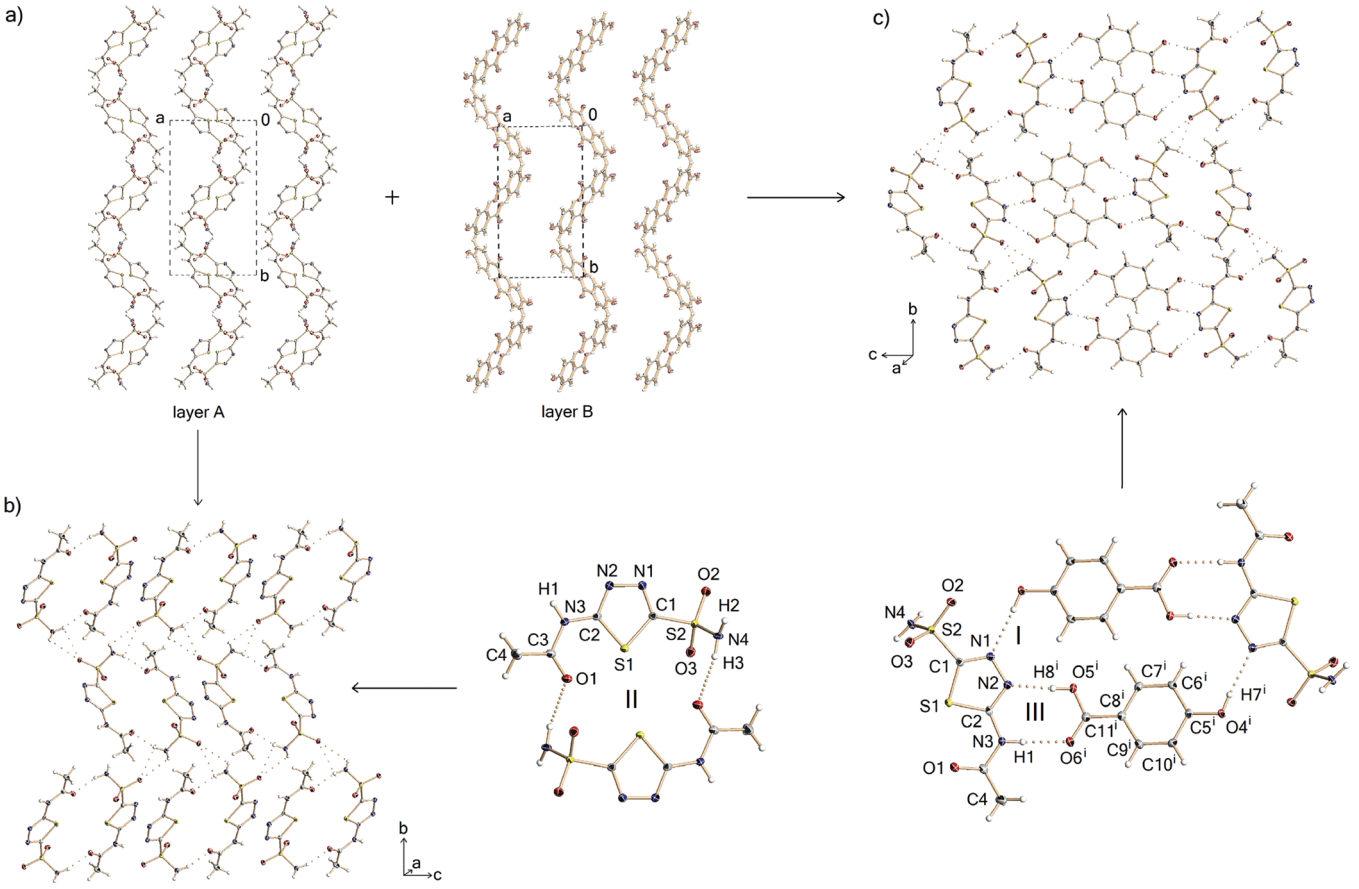

Figure 8. (a, b) In the crystal lattice of **ACZ-4HBA** alternating undulated layers of ACZ (layer A) and 4HBA molecules (layer B) are identified, which are (c) linked between each other through motifs **I** and **III** to give a 3D hydrogen bonded network. Symmetry operator: (i) $2 - x, -y, 1 - z$. Displacement ellipsoids are drawn at the 50% probability level and H atoms are shown as small spheres of arbitrary radii.

supported by the integrated ^{1}H NMR spectrum of the sample prepared by the RC method (Figure S6). A comparison of the XRPD patterns in Figure 5f,g shows that this new phase is stable in a capped vial at ambient conditions at least for four months; however, when stirred in water, the sample rehydrates (Figure 5h).

Co-Crystal Phase Stability Assays. In order to evaluate the solid-phase stability of co-crystals **ACZ-4HBA** and **ACZ-NA-H$_2$O**, samples of each phase were exposed to water at different physiological pH values, in order to examine if they transform to ACZ. For this purpose 25 mg samples of the co-crystals were stirred for 16 and 72 h in 100 μL of deionized water, and buffer solutions were adjusted to physiological pH values of 1.2, 4.5, and 6.8. Comparison of the XRPD patterns given in Figures S7 and 6 with the previously established patterns of the co-crystal (Figures 1 and 2) show that only **ACZ-4HBA** is stable, at least for 72 h, over the whole pH range examined. The XRPD pattern of **ACZ-NA-H$_2$O** recorded after exposition to water for 16 h indicated the presence of small quantities of **ACZ** (Figure 6c). When the experiment was prolonged to 72 h the transformation to ACZ increased significantly. Furthermore, the degree of transformation of **ACZ-NA-H$_2$O** to **ACZ** was found to be pH-dependent (Figure 6d−g). As already mentioned above, the dehydrated sample of this co-crystal, **ACZ-NA**, is completely rehydrated when stirred in deionized water (Figure 5h).

Competition Experiment for ACZ. In an attempt to carry out a competition experiment between **4HBA** and **NA** for **ACZ**, a 1:1:1 stoichiometric mixture of these reagents was ground mechanically in the presence of 1 drop of acetonitrile and water, respectively. In both cases a new solid phase was identified, which resulted in co-crystal **NA-4HBA** (1:1). This phase has been prepared also by SDG and NG in the absence of **ACZ**. Since this co-crystal has not been reported earlier, it has been characterized by XRPD (Figure S8), IR spectroscopy (Figure S9, Table 2), DSC-TGA (Figure S10, Table 3), and single-crystal X-ray diffraction analysis. As for **ACZ-4HBA**, the spectroscopic and structural data prove that also this phase is a true solvent-free co-crystal and not a salt (vide infra).

Single-Crystal Diffraction Analysis. Single co-crystals of **ACZ-4HBA** and **ACZ-NA-H$_2$O** could be grown only from solutions containing an excess of the co-crystal former (1:3 and 1:4, respectively); however, for **ACZ-4HBA** only crystal mixtures of **ACZ** and the corresponding co-crystal were obtained, which could be separated manually due to their different shapes (Figure 7). This phenomenon is common for solutions containing components with different solubilities and has been explained by the corresponding phase solubility diagram. For these cases, typically a rotation of the relatively small region, in which the co-crystal is the stable phase, toward the axis of the co-crystal former is found.[15g,h,25]

On the contrary, the generation of the **NA-4HBA** co-crystals could be performed straightforward from the 1:1 mixture of the components in acetone and they were isolated in pure form.

The most relevant crystallographic data of **ACZ-4HBA**, **ACZ-NA-H$_2$O**, and **NA-4HBA** are listed in Table 4. Co-crystals with **ACZ** have been collected both at room and at low temperature (293 and 100 K) in order to verify if a phase-

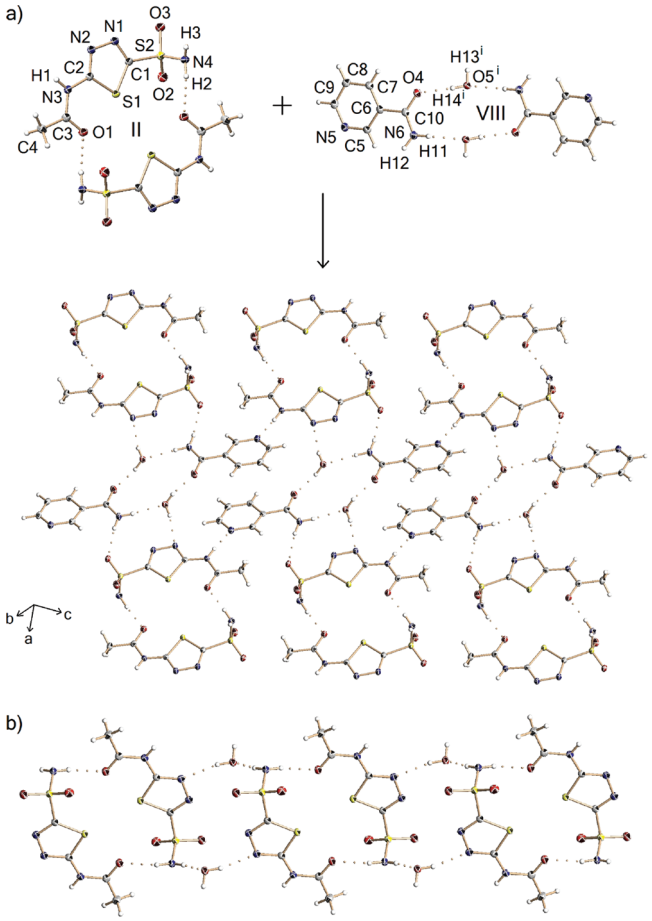

Figure 9. (a) In the crystal lattice of **ACZ-NA-H_2O** dimeric units containing ACZ and NA molecules are linked to 2D hydrogen bonded layers, which are (b) further connected through $N_{sulfonamide}-H\cdots O_w$ interactions to give an overall 3D hydrogen bonded network. Symmetry operator: (i) $-x, 1-y, 1-z$. Displacement ellipsoids are drawn at the 50% probability level and H atoms are shown as small spheres of arbitrary radii.

transition occurred and to visualize the extent of variations in the hydrogen-bonding geometries due to the temperature difference of 173 K. Interestingly, in both cases only very slight changes in the bonding parameters could be observed, indicating that the crystal structures are quite compact. Table S1 shows that, as expected, the D···A distances diminish upon lowering the data collection temperature; however, the values decrease less than 0.05 Å for **ACZ-4HBA** and 0.03 Å for **ACZ-NA-H_2O**. The corresponding maximum variations of the DHA bond angles are 3 and 4°, respectively. Scheme 2 summarizes the different hydrogen bonding motifs found in **ACZ-4HBA** (motifs **I**−**IV**), **ACZ-NA-H_2O** (motifs **V**−**VIII**), and **NA-4HBA** (motifs **IX**−**X**, Scheme 2).

Acetazolamide-4-hydroxybenzoic Acid (1:1). The asymmetric unit of **ACZ-4HBA** contains one molecule of each component confirming the 1:1 stoichiometry of the co-crystal. When viewed along axis *c*, two types of undulated layers can be identified, which are organized in the ABABAB... sequence typical for *hcp* structures. The A-layers contain only ACZ molecules, which are linked via the sulfonamide and acetamide groups through $N_{sulfonamide}-H\cdots O_{acetamide}$ and bifurcated $N_{sulfonamide}-H\cdots O_{sulfonamide}$ interactions (see motifs **II** and **IV** in Scheme 2). Motif **II** is also found in the crystal lattice of acetazolamide form A, and the bonding geometries are very similar.[9a,d] The B layers are formed by the co-crystal former, but interestingly, there are no direct hydrogen bonding interactions between the 4HBA units, which in neat **4HBA** are linked through homodimeric COOH···HOOC and OH···OH interactions.[26] This is because both the carboxyl and the hydroxyl functions interact through O−H···N and N−H···O hydrogen bonds with the thiadiazole and acetamido groups of ACZ molecules in neighboring A-layers (see motifs **I**, **III**, and **IV** in Scheme 2), thus generating a 3D hydrogen bonded network (Table S1, Figure 8). The double-bridged heterodimeric synthon C(N)NH···HOOC (**III**) substitutes the dominating homodimeric C(N)NH···HN(N)C synthon in forms A and B of neat **ACZ**.[9a,c,d] The formation of the heterodimeric C(N)-NH···HOOC synthon instead of the C(N)NH···HN(N)C homodimeric motif has been observed also for a series of co-crystals derived from sulfathiazole and related sulfadrugs.[3d,27]

Motifs **I** and **III** resemble two well-known synthons from traditional crystal engineering. The O−H···N motif **I** is typically found in co-crystals formed between pyridine and alcohols,[28] and motif **III** is structurally related to the heterosynthons formed between 2-aminopyridine derivatives and carboxylic acids.[29] It is well-known that the formation of double-bridged heterosynthons is frequently preferred over the formation of the corresponding homosynthons.[28] Therefore, it is not surprising to find that **4HBA** is an ideal co-crystal former for **ACZ**.

The X-ray structural data confirm also the observations from the IR spectra that **ACZ-4HBA** is indeed a co-crystal and not a salt. In deprotonated benzoic acids with delocalized carboxylate functions, the C−O distance in the carboxylate group is approximately 1.25 Å; otherwise, the average C−O and C═O distances are 1.31 Å and 1.21 Å, respectively.[15j,24] For **ACZ-4HBA** the C−O and C═O bond lengths at $T = 293$ K were 1.320(3) and 1.217(3) Å, respectively, confirming the formation of a true co-crystal.

Acetazolamide-Nicotinamide Monohydrate (1:1:1). The asymmetric unit of **ACZ-NA-H_2O** contains one molecule of each ACZ and NA plus one molecule of water, confirming the 1:1:1 stoichiometry of the co-crystal monohydrate (Figure 9). Similar to the crystal structures of **ACZ-form A** and **ACZ-4HBA** the ACZ molecules are connected to dimeric units through $N_{sulfonamide}-H\cdots O_{acetamide}$ interactions (motif **II**). The NA molecules form a water-expanded homodimeric motif through $N-H\cdots O_w$ and $O_w-H\cdots O_{carboxamide}$ hydrogen bonds (motif **VIII**). The ACZ and NA dimeric units are linked to each other through $N_{NA}-H\cdots O_{sulfonamide}$, $O_w-H\cdots N_{thiadiazole}$, and $N_{ACZ\text{-}acetamide}-H\cdots N_{pyr}$ interactions (motifs **V** and **VI**) to give the 2D hydrogen bonded layer shown in Figure 9a. These 2D layers are further connected through $N_{sulfonamide}-H\cdots O_w$ interactions (motif **VII**) to give an overall 3D hydrogen bonded network (Table S1, Scheme 2). The latter interactions generate hydrogen bonded chains of ACZ dimers linked by water molecules running parallel to the *ab* diagonal (Figure 9b). This connectivity indicates that each water molecule participates in a total of four hydrogen bonds, thus playing a key role in the stabilization of this crystal structure.

Nicotinamide-4-hydroxybenzoic Acid (1:1). The asymmetric unit of **NA-4HBA** contains one molecule of each component confirming the 1:1 stoichiometry of the co-crystal. The supramolecular organization of the NA and 4HBA molecules in the crystal structure of **NA-4HBA** and the resulting hydrogen bonding pattern can be seen from Figure 10. The two components form the well-known COOH···amide and $O-H\cdots N_{pyr}$ heterosyntons **IX**[29,30] and **X**[28] to give 1D infinite double chains running along the *ac* diagonal (Table S1, Scheme 2). The 3D

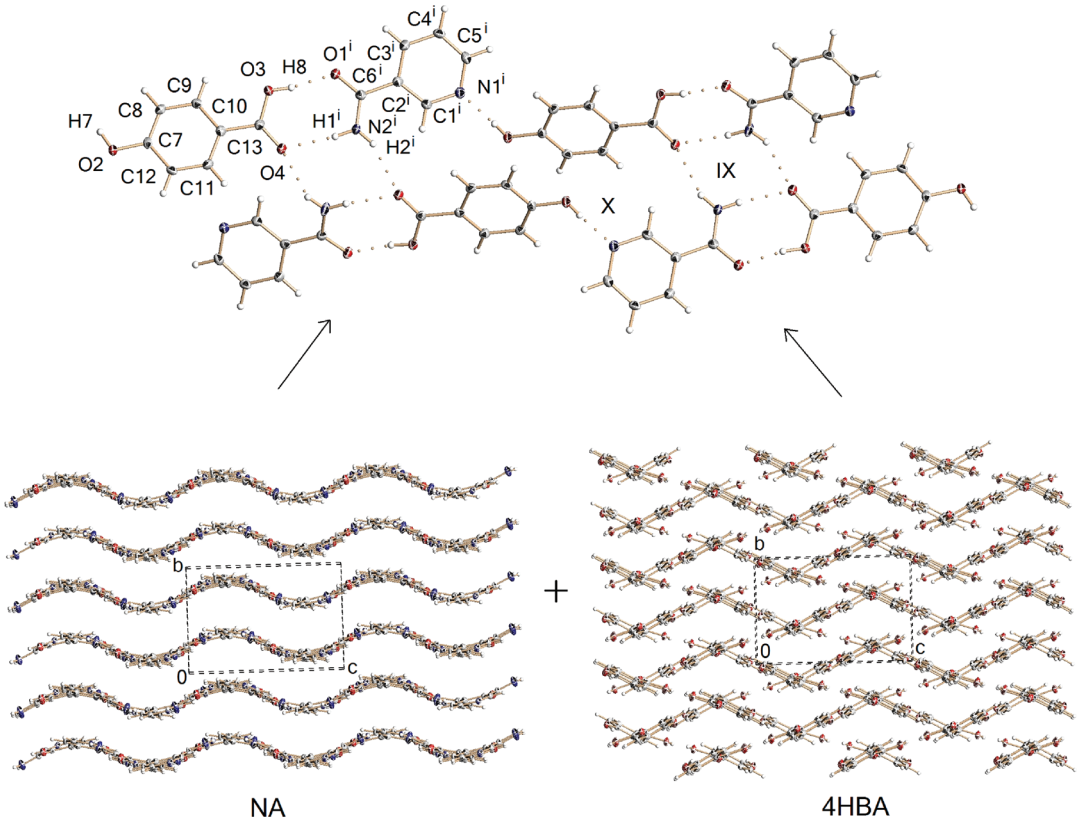

Figure 10. The components in the crystal lattice of co-crystal **NA-4HBA** are connected through motifs **IX** and **X** to 1D double chains, which are further linked through two different C−H···O contacts. The supramolecular organization of the individual NA and 4HBA molecules is also indicated. Symmetry operator: (i) $2 - x$, y, $1.5 - z$. Displacement ellipsoids are drawn at the 50% probability level and H atoms are shown as small spheres of arbitrary radii.

arrangement is further stabilized by two different C−H···O contacts (C3−H···O1 = 2.57 Å; C9−H···O2 = 2.67 Å). Interestingly, while motifs **IX** and **X** are both observed also in the **INA-4HBA** co-crystal,[31] in **NA-3HBA**[30d] and **NA-2HBA**[18b] only the O−H···N_{pyr} motif **X** is found.

Analysis of Hydrogen Bonding Sites in Acetazolamide. In the molecular structure of ACZ, three sites capable of forming hydrogen bonding interactions can be identified: (i) the acetamide group, (ii) the sulfonamide group, and (iii) the thiadiazole ring. The acetamide and sulfonamide moieties contain at least one hydrogen bond donor and acceptor, while the thiadiazole ring can act only as hydrogen bond acceptor. Overall, ACZ contains three N−H donor sites, but three oxygen and two nitrogen acceptors, which might indicate that co-crystal formers with an excess of donor functions are good candidates for co-crystal formation with this API.

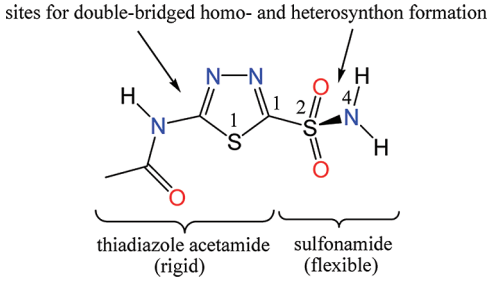

Figure 11 shows the molecular conformations of ACZ found in the crystal structures of forms A and B,[9a,c,d] and the

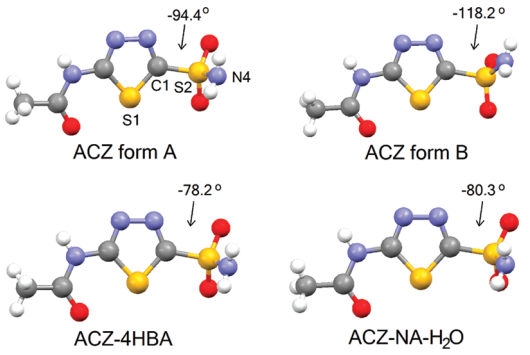

Figure 11. Molecular conformations of ACZ in the crystal structures of **ACZ form A**,[9a,d] **ACZ form B**,[9c] **ACZ-4HBA**, and **ACZ-NA-H_2O**. N4−S2−C1−S1 torsion angles are indicated. Note: Only molecules with negative torsion angles are shown.

co-crystals described herein. Interestingly, due to an intramolecular O···S interaction in all cases the acetamide function has *Z*-configuration,[9d] which explains that double-bridged COOH···amide and amide···amide synthons with ACZ are absent in the co-crystals examined herein, albeit these synthons are relatively robust.[29,30] Further, in all four molecular structures the acetamide moiety is almost coplanar with the thiadiazole ring, as indicated by the small angles formed between the mean planes of these units (1.8−4.9° at T = 293 K). This can be attributed to delocalization of the N_{amide} lone pair, thus making the whole thiadiazole acetamide fragment relatively rigid. On the contrary, the sulfonamide moiety is

more flexible and rotational conformers arise both from rotation around the N4−S2 and C1−S2 bonds. This is illustrated by the N4−S2−C1−S1 torsion angles with values ranging from −78.2 to −118.2° and +78.2 to +118.2° (T = 293 K).[32]

These structural details demonstrate that ACZ possesses two potential sites for the formation of double-bridged homo- and heterosynthons, the carboxamidine (C(N)NH) group on the thiadiazole acetamide fragment and the sulfonamide group. Interestingly, in three of the four crystal structures mentioned above the C(N)NH unit is indeed involved in the formation of such synthons, which are homodimeric in **ACZ forms A** and **B**, and heterodimeric in **ACZ-4HBA**. The homodimeric C(N)NH···HN(N)C synthon also is stable in solution as shown by cold spray ionization (CSI) mass spectrometry of ACZ in methanol[9d] and also is formed in the solid state by sulfathiazole and related sulfadrugs.[3d,27] Although the sulfonamide homodimer is a well-known synthon,[29,33] in the present structures it is only observed in **ACZ form A**. In this polymorph, the ACZ molecules dimerize further to motif **II** through $N_{sulfonamide}$−H···$O_{acetamide}$ interactions,[9a,d] which also is present in **ACZ-4HBA** and **ACZ-NA-H_2O**. In **ACZ-form B** the sulfonamide groups are involved in monomeric $N_{sulfonamide}$−H···$O_{sulfonamide}$ and $N_{sulfonamide}$−H···$N_{thiadiazole}$ contacts.[9c] A further interesting aspect is that in all four crystal structures O−H···O interactions with ACZ are completely absent and only O−H···N, N−H···O, and N−H···N interactions are occurring.

4. Conclusions

The present study has shown that ACZ can form co-crystals with carboxylic acids and carboxamides via a series of different hydrogen bonds that include the double-bridged C(N)NH···HOOC synthon as well as N−H···N, O−H···N, and N−H···O interactions. Interestingly, in the two structurally characterized co-crystals with ACZ the API was incorporated into the crystal structure in the form of a dimeric fragment that is found also in the crystal structure of the ACZ polymorph employed for the grinding experiments.

As indicated by the co-crystal phase stability experiments, solid samples of **ACZ-4HBA** do not transform to ACZ when exposed to water at different physiological pH values; however, **ACZ-NA-H_2O** transforms slowly into ACZ. A further interesting result is that **ACZ-NA-H_2O** can be dehydrated by thermal treatment to give a new co-crystalline solid phase of the composition **ACZ-NA**, which is stable at ambient conditions for several months but transforms to the corresponding hydrate upon stirring in water.

Acknowledgment. This work received support from Consejo Nacional de Ciencia y Tecnologia (CONACyT) in form of a postgraduate fellowship for J.I.A.-G. and through project No. CB2007-83440.

Supporting Information Available: DSC-TGA graphs for **ACZ**, **ACZ-4HBA**, **ACZ-NA-H_2O**, and **NA-4HBA**. IR spectra for **ACZ-NA-H_2O**, **NA-4HBA**, and **ACZ-NA-H_2O** (before and after thermal treatment). ^{1}H NMR spectra of (a) **ACZ**, (b) **NA**, and (c) **ACZ-NA**. XRPD patterns for the co-crystal phase stability assays of **ACZ-4HBA** in water at different physiological pH values. XRPD patterns for **NA-4HBA**. Table with hydrogen bonding geometries for compounds **ACZ-4HBA**, **ACZ-NA-H_2O**, and **NA-4HBA**. This material is available free of charge via the Internet at http://pubs.acs.org.

References

(1) (a) Morissette, S. L.; Almarsson, Ö.; Peterson, M. L.; Remenar, J. F.; Read, M. J.; Lemmo, A. V.; Ellis, S.; Cima, M. J.; Gardner, C. R. *Adv. Drug Delivery Rev.* **2004**, *56*, 275–300. (b) Blagden, N.; de Matas, M.; Gavan, P. T.; York, P. *Adv. Drug Delivery Rev.* **2007**, *59*, 617–630. (c) Chow, K.; Tong, H. H. Y.; Lum, S.; Chow, A. H. L. *J. Pharm. Sci.* **2008**, *97*, 2855–2877. (d) Shan, N.; Zaworotko, M. J. *Drug Discovery Today* **2008**, *13*, 440–446.

(2) (a) Byrn, S. R.; Pfeiffer, R. R.; Stowell, J. G. *Solid State Chemistry of Drugs*, 2nd ed.; West Lafayette, IN: SSCI Inc., 1999. (b) Datta, S.; Grant, D. J. W. *Nat. Rev. Drug Discovery* **2004**, *3*, 42–57.

(3) For feature articles and reviews of pharmaceutical co-crystals see (a) Almarsson, Ö.; Zawarotko, M. J. *Chem. Commun.* **2004**, 1889–1896. (b) Bernstein, J. *Chem. Commun.* **2005**, 5007–5012. (c) Vishweshwar, P.; McMahon, J. A.; Bis, J. A.; Zaworotko, M. J. *J. Pharm. Sci.* **2006**, *95*, 499–516. (d) Caira, M. R. *Mol. Pharmaceutics* **2007**, *4*, 310–316. (e) Blagden, N.; Berry, D. J.; Parkin, A.; Javed, H.; Ibrahim, A.; Gavan, P. T.; De Matos, L. L.; Seaton, C. C. *New. J. Chem.* **2008**, *32*, 1659–1672. (f) Friščić, T.; Jones, W. *Cryst. Growth Des.* **2009**, *9*, 1621–1637. (g) Schultheiss, N.; Newman, A. *Cryst. Growth Des.* **2009**, *9*, 2950–2967. (h) Childs, S. L.; Zaworotko, M. J. *Cryst. Growth Des.* **2009**, *9*, 4208–4211. (i) Stahly, G. P. *Cryst. Growth Des.* **2009**, *9*, 4212–4229.

(4) For recent reports on pharmaceutical co-crystals see (a) Guo, K.; Sadiq, G.; Seaton, C.; Davey, R.; Yin, Q. *Cryst. Growth Des.* **2010**, *10*, 268–273. (b) Habgood, M.; Deij, M. A.; Mazurek, J.; Price., S. L.; ter Horst, J. H. *Cryst. Growth Des.* **2010**, *10*, 903–912. (c) Urbanus, J.; Roelands, C. P. M.; Verdoes, D.; Jansens, P. J.; ter Horst, J. H. *Cryst. Growth Des.* **2010**, *10*, 1171–1179. (d) Stevens, J. S.; Byard, S. J.; Schroeder, S. L. M. *Cryst. Growth Des.* **2010**, *10*, 1419–1434. (e) Lee, T.; Wang, P. Y. *Cryst. Growth Des.* **2010**, *10*, 1435–1442. (f) Liao, X.; Gautam, M.; Grill, A.; Zhu, H. J. *J. Pharm. Sci.* **2010**, *99*, 246–254. (g) Schultheiss, N.; Lorimer, K.; Wolfe, S.; Desper, J. *CrystEngComm* **2010**, *12*, 742–749.

(5) For recent reviews on crystal engineering see (a) Desiraju, G. R. *Angew. Chem., Int. Ed.* **2007**, *46*, 8342–8356. (b) Aakeröy, C. B.; Champness, N. R.; Janiak, C. *CrystEngComm* **2010**, *12*, 22–43.

(6) Traks, A. V. *Mol. Pharmaceutics* **2007**, *4*, 301–309.

(7) (a) Chakravarty, S.; Kannan, K. K. *J. Mol. Biol.* **1994**, *243*, 298–309. (b) Nair, S. K.; Krebs, J. F.; Christianson, D. W.; Fierke, C. A. *Biochemistry* **1995**, *34*, 3981–3989.

(8) (a) Kasim, N. A.; Whitehouse, M.; Ramachandran, C.; Bermejo, M.; Lennernäs, H.; Hussain, A. S.; Junginger, H. E.; Stavchansky, S. A.; Midha, K. K.; Shah, V. P.; Amidon, G. L. *Mol. Pharmaceutics* **2004**, *1*, 85–96. (b) Ono N.; Ushijima I. Patent JP2009269856(A), 2009. (c) Swenson E. R. Patent US2009131490(A1), 2009.

(9) (a) Mathew, M.; Palenik, G. J. *J. Chem. Soc., Perkin Trans. 2* **1974**, 532–536. (b) Umeda, T.; Ohnishi, N.; Yokoyama, T.; Kuroda, T.; Kita, Y.; Kuroda, K.; Tatsumi, E.; Matsuda, Y. *Chem. Pharm. Bull.* **1985**, *33*, 3422–3428. (c) Griesser, U. J.; Burger, A.; Mereiter, K. *J. Pharm. Sci.* **1997**, *86*, 352–358. (d) Nagao, Y.; Honjo, T.; Iimori, H.; Goto, S.; Sano, S.; Shiro, M.; Yamaguchi, K.; Sei, Y. *Tetrahedron Lett.* **2004**, *45*, 8757–8761. (e) Baraldi, C.; Gamberini, M. C.; Tinti, A.; Palazzoli, F.; Ferioli, V. *J. Mol. Struct.* **2009**, *918*, 88–96.

(10) (a) Duffel, M. W.; Ing, I. S.; Segarra, T. M.; Dixson, J. A.; Barfknecht, C. F.; Schoenwald, R. D. *J. Med. Chem.* **1986**, *29*, 1488–1494. (b) Parasrampuria, J.; Gupta, V. D. *J. Pharm. Sci.* **1990**, *79*, 835–836. (c) El-Gazayerly, O. N.; Hikal, A. H. *Int. J. Pharm.* **1997**, *158*, 121–127. (d) Haznedar, S.; Dortunç, B. *Int. J. Pharm.* **2004**, *269*, 131–140. (e) Pudipeddi, M.; Serajuddin, A. T. M. *J. Pharm. Sci.* **2005**, *94*, 929–939. (f) Granero, G. E.; Longhi, M. R.; Becker, C.; Junginger, H. E.; Kopp, S.; Midha, K. K.; Shah, V. P.; Stavchansky, S.; Dressman, J. B.; Barends, D. M. *J. Pharm. Sci.* **2008**, *97*, 3691–3699.

(11) (a) *SMART: Molecular Analysis Research Tool*, Versions 5.057 and 5 0.618; Bruker Analytical X-ray Systems: Madison, WI, 1997 and 2000. (b) *SAINT + NT*, Versions 6.01 and 6.04; Bruker Analytical X-ray Systems: Madison, WI, 1999 and 2001. (c) Sheldrick, G. M. *SHELX86, Program for Crystal Structure Solution*; University of Göttingen: Germany, 1986. (d) SHELXTL-NT, Versions 5.10 and 6.10; Bruker Analytical X-ray Systems: Madison, WI, 1999 and 2000.

(12) Farrugia, L. J. *J. Appl. Crystallogr.* **1999**, *32*, 837–838.

(13) GRAS = Generally Regarded As Safe. This list is published by the U.S. Food and Drug Administration (FDA).

(14) (a) Bučar, D.-K.; Henry, R. F.; Lou, X.; Duerst, R. W.; MacGillivray, L. R.; Zhang, G. G. Z. *Cryst. Growth Des.* **2008**, *8*, 3032–3037. (b) Good, D. J.; Rodríguez-Hornedo, N. *Cryst. Growth Des.* **2010**, *10*, 1028–1032.

(15) (a) Fleischman, S. G.; Kuduva, S. S.; McMahon, J. A.; Moulton, B.; Bailey Walsh, R. D.; Rodríguez-Hornedo, N.; Zaworotko, M. J. *Cryst. Growth Des.* **2003**, *3*, 909–919. (b) Rodríguez-Hornedo, N.; Nehm, S. J.; Seefeldt, K. F.; Pagán-Torres, Y.; Falkiewicz, C. J. *Mol. Pharmaceutics* **2006**, *3*, 362–367. (c) Hickey, M. B.; Peterson, M. L.; Scoppettuolo, L. A.; Morrisette, S. L.; Vetter, A.; Guzmán, H.; Remenar, J. F.; Zhang, Z.; Tawa, M. D.; Haley, S.; Zaworotko, M. J.; Almarsson, Ö. *Eur. J. Pharm. Biopharm.* **2007**, *67*, 112–119. (d) Jayasankar, A.; Good, D. J.; Rodríguez-Hornedo, N. *Mol. Pharmaceutics* **2007**, *4*, 360–372. (e) Zhang, G. G. Z.; Henry, R. F.; Borchardt, T. B.; Lou, X. *J. Pharm. Sci.* **2007**, *96*, 990–995. (f) Seefeldt, K.; Miller, J.; Alvarez-Núñez, F.; Rodríguez-Hornedo, N. *J. Pharm. Sci.* **2007**, *96*, 1147–1158. (g) Childs, S. L.; Rodríguez-Hornedo, N.; Reddy, L. S.; Jayasankar, A.; Maheshwari, C.; McCausland, L.; Shipplett, R.; Stahly, B. C. *CrystEngComm* **2008**, *10*, 856–864. (h) ter Horst, J. H.; Cains, P. W. *Cryst. Growth Des.* **2008**, *8*, 2537–2542. (i) Childs, S. L.; Wood, P. A.; Rodríguez-Hornedo, N.; Reddy, L. S.; Hardcastle, K. I. *Cryst. Growth Des.* **2009**, *9*, 1869–1888. (j) Good, D. J.; Rodríguez-Hornedo, N. *Cryst. Growth Des.* **2009**, *9*, 2252–2264. (k) Chieng, N.; Hubert, M.; Saville, D.; Rades, T.; Aaltonen, J. *Cryst. Growth Des.* **2009**, *9*, 2377–2386. (l) Maheshwari, C.; Jayasankar, A.; Khan, N. A.; Amidon, G. E.; Rodríguez-Hornedo, N. *CrystEngComm* **2009**, *11*, 493–500.

(16) Remenar, J. F.; Peterson, M. L.; Stephens, P. W.; Zhang, Z.; Zimenkov, Y.; Hickey, M. B. *Mol. Pharmaceutics* **2007**, *4*, 386–400.

(17) Nicoli, S.; Bilzi, S.; Santi, P.; Caira, M. R.; Li, J.; Bettini, R. *J. Pharm. Sci.* **2008**, *97*, 4830–4839.

(18) (a) Oberoi, L. M.; Alexander, K. S.; Riga, A. T. *J. Pharm. Sci.* **2005**, *94*, 93–101. (b) Berry, D. J.; Seaton, C. C.; Clegg, W.; Harrington, R. W.; Coles, S. J.; Horton, P. N.; Hursthouse, M. B.; Storey, R.; Jones, W.; Friščić, T.; Blagden, N. *Cryst. Growth Des.* **2008**, *8*, 1697–1712.

(19) Childs, S. L.; Hardcastle, K. I. *Cryst. Growth Des.* **2007**, *7*, 1291–1304.

(20) Childs, S. L.; Stahly, G. P.; Park, A. *Mol. Pharmaceutics* **2007**, *4*, 323–338.

(21) (a) Shan, N.; Toda, F.; Jones, W. *Chem. Commun.* **2002**, 2372–2373. (b) Trask, A. V.; Motherwell, W. D. S.; Jones, W. *Chem. Commun.* **2004**, 890–891.

(22) (a) Seaton, C. C.; Parkin, A.; Wilson, C. C.; Bladgen, N. *Cryst. Growth Des.* **2009**, *9*, 47–56. (b) Kashino, S.; Tateno, S.; Tanabe, H.; Haisa, M.; Katsube, Y. *Acta Crystallogr. C* **1991**, *47*, 2236–2239. (c) Perlovich, G. L.; Hansen, L. Kr.; Volkova, T. V.; Mirza, S.; Manin, A. N.; Bauer-Brandl, A. *Cryst. Growth Des.* **2007**, *7*, 2643–2648.

(23) Hesse, M.; Meier, H.; Zeeh, B. *Spektroskopische Methoden in der Organischen Chemie*, 3rd ed.; Georg Thieme Verlag: New York, 1987.

(24) (a) Bis, J. A.; Zaworotko, M. J. *Cryst. Growth Des.* **2005**, *5*, 1169–1179. (b) Bhogala, B. R.; Basavoju, S.; Nangia, A. *CrystEngComm* **2005**, *7*, 551–562. (c) Reddy, L. S.; Bethune, S. J.; Kampf, J. W.; Rodríguez-Hornedo, N. *Cryst. Growth Des.* **2009**, *9*, 378–385.

(25) (a) Chiarella, R. A.; Davey, R. J.; Peterson, M. L. *Cryst. Growth Des.* **2007**, *7*, 1223–1226. (b) Jayasankar, A.; Reddy, L. S.; Bethune, S. J.; Rodríguez-Hornedo, N. *Cryst. Growth Des.* **2009**, *9*, 889–897.

(26) Heath, E. A.; Singh, P.; Ebisuzaki, Y. *Acta Crystallogr.* **1992**, *C48*, 1960–1965.

(27) (a) Bingham, A. L.; Hughes, D. S.; Hursthouse, M. B.; Lancaster, R. W.; Tavener, S.; Threlfall, T. L. *Chem. Commun.* **2001**, 603–604. (b) Adsmond, D. A.; Grant, D. J. W. *J. Pharm. Sci.* **2002**, *90*, 2058–2077. (c) Stanton, M. K.; Bak, A. *Cryst. Growth Des.* **2008**, *8*, 3856–3862. (d) Stanton, M. K.; Tufekcic, S.; Morgan, C.; Bak, A. *Cryst. Growth Des.* **2009**, *9*, 1344–1352.

(28) (a) Bis, J. A.; Vishweshwar, P.; Weyna, D. R.; Zaworotko, M. J. *Mol. Pharmaceutics* **2007**, *4*, 401–416. (b) Shattock, T. R.; Arora, K. K.; Vishweshwar, P.; Zaworotko, M. J. *Cryst. Growth Des.* **2008**, *8*, 4533–4545. (c) Weyna, D. R.; Shattock, T.; Vishweshwar, P.; Zaworotko, M. J. *Cryst. Growth Des.* **2009**, *9*, 1106–1123.

(29) (a) Allen, F. H.; Motherwell, W. D. S.; Raithby, P. R.; Shields, G. P.; Taylor, R. *New. J. Chem.* **1999**, 25–34. (b) Bhatt, P. M.; Azim, Y.; Thakur, T. S.; Desiraju, G. R. *Cryst. Growth Des.* **2009**, *9*, 951–957.

(30) (a) Aakeröy, C. B.; Beatty, A. M.; Helfrich, B. A. *J. Am. Chem. Soc.* **2002**, *124*, 14425–14432. (b) Aakeröy, C. B.; Beatty, A. M.; Helfrich, B. A.; Nieuwenhuyzen, M. *Cryst. Growth Des.* **2003**, *3*, 159–165. (c) Aakeröy, C. B.; Desper, J.; Helfrich, B. A. *CrystEngComm* **2004**, *6*, 19–24. (d) McMahon, J. A.; Bis, J. A.; Vishweshwar, P.; Shattock, T. R.; McLaughlin, O. L.; Zawarotko, M. J. *Z. Kristallogr.* **2005**, *220*, 340–350.

(31) Vishweshwar, P.; Nangia, A.; Lynch, V. W. *CrystEngComm* **2003**, *5*, 164–168.

(32) The ACZ molecules in the crystal lattices of **ACZ form A**, **ACZ form B**, **ACZ-4HBA** and **ACZ-NA-H_2O** are related by inversion centers. Therefore, each crystal lattice contains two rotamers having N4−S2−C1−S1 torsion angles with opposite signs.

(33) Babu, N. J.; Cherukuvada, S.; Thakuria, R.; Nangia, A. *Cryst. Growth Des.* **2010**, *10*, 1979–1989.